Towards Photoferroic Materials by Design: Recent Progresses and Perspective

Castelli, Ivano E.; Olsen, Thomas; Chen, Yunzhong

Published in:
Journal of Physics: Energy

Link to article, DOI:
10.1088/2515-7655/ab428c

Publication date:
2020

Document Version
Publisher's PDF, also known as Version of record

JPhys Energy

PERSPECTIVE • OPEN ACCESS

Towards photoferroic materials by design: recent progress and perspectives

JPhys Energy

PERSPECTIVE

Towards photoferroic materials by design: recent progress and perspectives

Ivano E Castelli[1,4], **Thomas Olsen**[2,4] **and Yunzhong Chen**[3,4]

[1] Department of Energy Conversion and Storage, Technical University of Denmark, DK-2800 Kgs. Lyngby, Denmark
[2] Department of Physics, Technical University of Denmark, DK-2800 Kgs. Lyngby, Denmark
[3] Department of Energy Conversion and Storage, Technical University of Denmark, DK-4000 Roskilde, Denmark
[4] Authors to whom any correspondence should be addressed.

E-mail: ivca@dtu.dk, tolsen@fysik.dtu.dk and yunc@dtu.dk

Keywords: photoferroics, perovskites, photovoltaics, high-throughput screening

PUBLISHED
27 November 2019

Abstract

The use of photoferroic materials that combine ferroelectric and light-harvesting properties in a photovoltaic device is a promising route to significantly improving the efficiency of solar cells. These materials do not require the formation of a p−n junction and can produce photovoltages well above the value of the band gap, because of spontaneous intrinsic polarization and the formation of domain walls. From this perspective, we discuss the recent experimental progress and challenges regarding the synthesis of these materials and the theoretical discovery of novel photoferroic materials using a high-throughput approach.

1. Introduction

The increase in energy demand and the demand for a society independent from fossil fuels necessitate the development of novel sources of green energy. Photovoltaics (PV) converts solar energy directly into electricity and is one of the dominant technologies for a green future. In a typical PV device, the incoming photon is absorbed by the photo-absorbing semiconducting layer, exciting an electron to the conduction band and thus generating an electron–hole (e–h) pair. These pairs are afterwards separated by a p–n junction, which results in a voltage difference across the junction (figure 1(a)). The electricity generated can then be connected to the grid, stored in batteries or used to create fuels by means of electrolyzers. Another technology that relies on harvesting solar light is a photoelectrochemical water-splitting (PEC) device, in which the e–h pairs are used to split water into hydrogen and oxygen molecules [1]. A fundamental requirement for both technologies is the efficient absorption of a significant part of the solar spectrum as well as a slow rate of e–h recombination and stability of the photoactive material. The maximum theoretical efficiency achievable by a single material in a PV device is around 33%, which corresponds to a band gap of around 1.1 eV, under solar irradiation and taking into account the possible thermodynamic losses. Many solutions have been proposed to break this limit, called the Schockley–Queisser (SQ) limit [2]. These include the development of cells based on multi-junctions, solar concentrators, high purity and thin-film materials. The common requirement of these solutions is that the maximum photovoltage obtainable by the device corresponds to the sum of the band gaps of the materials involved [3]. According to the annual summary of the progress of materials and device constructions towards achieving the highest efficiencies of PV cells [4], organometal halide perovskites have recently been suggested as emerging materials for PV devices because of their good light absorption properties, long lifetimes, and high mobility of the photogenerated charges [5]. However, issues like limited stability and toxicity (because of Pb content) have reduced their applicability in everyday devices [6].

Another emerging class of PV devices is based on ferroelectric materials for photoabsorption and is referred to as photoferroics [7]. This new type of PV device can, in principle, achieve photovoltages larger than the band gap, thus breaking the SQ limit. These materials not only absorb sunlight, but also exhibit an intrinsic

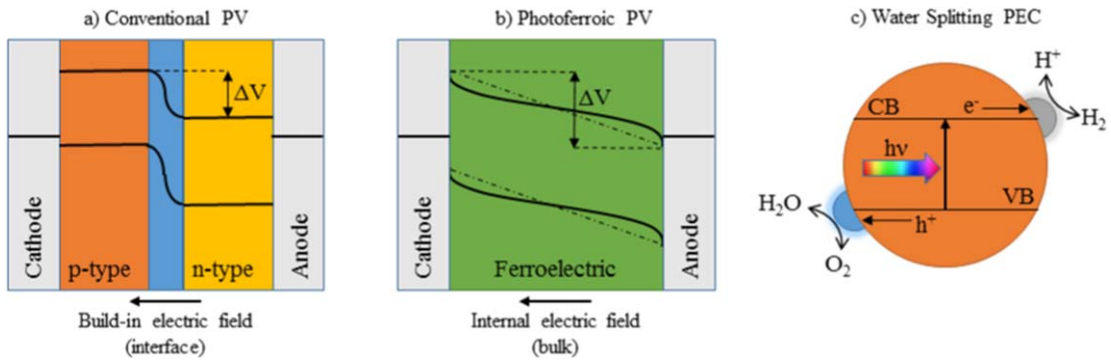

Figure 1. Illustration of a conventional PV cell based on a p–n junction (a), where the splitting of e–h pairs is due to the electric field built at the interface (ΔV indicates the potential difference), and on photoferroic devices, for which the splitting of photogenerated charges is enhanced by internal polarization (b). The scheme of a photoelectrochemical cell is also shown (c).

polarization below a critical temperature (the Curie temperature T_c) that gives rise to a depolarization field ($\mathbf{E}_{dp} = -\mathbf{P}/\epsilon_0$), which separates the e–h pairs directly without need for a p–n junction. More precisely, the presence of a polar axis allows a second-order optical conductivity that can yield a DC current in response to the AC optical frequencies. This leads to a photovoltaic mechanism very different from the conventional solar cells based on p–n junctions, as shown in figure 1(b).

In a pristine ferroelectric material, the polarization field implies a built-in voltage difference across the samples that may become arbitrarily large, essentially depending on the size of the sample in the direction of the intrinsic polarization. However, in order to collect the photoexcited charge carriers the ferroelectric has to be connected to electrodes that will compensate the surface charges of the ferroelectric and inadvertently screen the depolarization field. For perfectly metallic electrodes the screening will be complete and the depolarization field and voltage difference vanish. However, in real devices the screening will always be incomplete and there will be a remnant depolarization field that drives the separation of electrons and holes in the ferroelectric. This will also result in charge depletion, band bending (as illustrated by the solid line in figure 1(b)) and Schottky barriers at the interfaces, similar to the case of conventional photovoltaics. The deviation for perfect metallic behavior in the electrodes can be described by the screening length l_s of the electrodes. Thus when the thickness d becomes much larger than the screening length l_s, the depolarization field becomes small. Model calculations of the depolarization field for a given set of dielectric constants and electrode screening length can be found in the literature [8, 9]. The efficiency of charge separation is thus expected to be largest for thin ferroelectric films, which may limit the proportion of solar light absorbed. There are several other limitations to the use of photoferroic materials in photovoltaic applications, as will be discussed later, and the experimental progress in the field has so far been rather limited. A list of the most recent emerging technologies for PV has recently been published [10].

Computational methods, in particular in the framework of density functional theory (DFT) [11, 12], have recently been used to design and discover novel materials with target properties for several applications, from topological insulators and ferromagnetic materials [13–15] to catalysts, batteries and solar energy conversion devices [16]. Two factors have contributed to this, namely the increase in computational power together with significant methodological improvements, which have made it possible to study more complex and realistic systems with good predictability of experimental results [17–19]. Efficient light-harvesting materials, for example, have been discovered thanks to high-throughput screening approaches [20–23]. In addition, recent progress in the first-principles discovery of new ferroelectrics could lead the way to a direct bottom-up design of high-yield photoferroic materials [24, 25].

From this perspective, we discuss the current status of photoferroic materials for solar light conversion and the challenges, in theory as well as experimentally, that need to be addressed to enable broader use of this technology. Most of the work on photoferroics is focused on perovskite oxides, because they exist in multiple phases (cubic, layered, double, ...) and with almost all chemical elements in the periodic table. They also show manifold properties from ferroelectricity and superconductivity to efficient light-harvesting and high stability [26]. This manuscript is organized as follows: in section 2, we report the most recent experimental progress; section 3 describes the theoretical background for photoferroic materials and their *in silico* discovery; and section 4 is an outlook on possible methods to solve the identified challenges.

Table 1. Summary of the fundamental properties of the some of the most recently studied single-layer ferroelectric thin-film solar cells: band gap (E_g [eV]), spontaneous polarization (P [μC cm^{-2}]), curie temperature (T_c [K]), photocurrent (J_{sc} [mA cm^{-2}]), incident wavelength (λ [nm]), solar cell power conversion efficiency (PCE) (η [%]).

Composition	Crystal symmetry	E_g	P	T_c	J_{sc}	λ	η	References
$BaTiO_3$	Tetragonal, P4mm	3.4	29	404	$2.5^{*}10^{-5}$	366	$1.4^{*}10^{-4}$	[36]
$PbZr_{1-x}Ti_xO_3$	Cubic, Pm–3m	3.9–4.4	82	723	$2.0^{*}10^{-7}$	633	$1.3^{*}10^{-7}$	[37]
$LiNbO_3$	Trigonal, R3c	3.78	72	1483	$1^{*}10^{-6}$	514.5	0.03	[38]
$BiFeO_3$	Rhombohedral, R3c	2.67	6.1 (bulk) 80–100 (films)	1103	1.5	AM1.5	0.17	[39]
Bi_2FeCrO_6	Rhombohedral, R3	1.4–2.1	80	485	11.7	AM1.5	3.3	[33]
$KBiFe_2O_5$	Orthorhombic, P21cn	1.6	3.73	780	0.015	254	—	[40]
$(K, Ba)(Ni, Nb)O_{3-\delta}$	Tetragonal, P4mm	1.1–3.8	19	673	0.004	543.5	—	[41]
$Bi_xMn_{1-x}O_3$	Monoclinic, C2	1.1	25	770	0.25	AM1.5	0.07	[42]
SbSI	Orthorhombic, Pna2	2.1	20	295	8.59	AM1.5	3.05	[29]

2. Recent experimental progress

Photoferroic materials combine the properties of light-harvesting materials and ferroelectrics in a single compound [27]. The concept dates back to the late 1970s, and SbSI is regarded as a prototypical ferroelectric semiconductor with a band gap of 1.9–2.0 eV and spontaneous polarization of ~25 μC cm^{-2} [28]. However, a solar cell based on SbSI was only reported recently with a very promising efficiency of 3%–4% under solar irradiation [29]. Photoferroic solar cells thus remain in their infancy.

Recently, due also to the success of halide perovskite solar cells, photoferroic perovskite materials have gained revived attention in the research community. Perovskite oxides, with a prototypical formula of ABO_3, are the most studied ferroelectric materials and have been used in light-harvesting devices. Their large band gap, which is the reason why they can exhibit large photovoltages, is also the cause of their poor power conversion efficiency, since only a small fraction of the solar spectrum is adsorbed and the photocurrent under visible light is small (~nA cm^{-2}) [30]. A good photoferroic material for visible light absorption should enable the ideal combination of an optical gap in the range of 1–2 eV, high electric polarization, suitable e–h mobility, and good stability [31]. Since 2009, $BiFeO_3$ (BFO)-based materials have been among the most commonly studied photoferroics [32]. BFO has a a band gap of around 2.2 eV, but for optimal photoferroic properties it is desirable to find materials with smaller band gaps. The double perovskite $Bi_2Fe_{1-x}Cr_xO_6$ (BFCO) exhibits a tunable band gap between 1.5 and 2.7 eV, depending on the Fe/Cr ratio, and such tunable properties could turn out to be highly promising for the design of novel photoferroic devices [29]. Moreover, power conversion efficiencies of 3.3% and 8.1% for Bi_2FeCrO_6 under AM 1.5 G irradiation (100 mW cm^{-2}) have been reported for a single-phase solar cell and thin-film solar cells in a multilayer configuration, respectively [33]. The high efficiency of BFCO solar cells was ascribed to their narrow direct band gap, which enhances light absorption. First-principles calculations have suggested that the excellent performance also lies in a more efficient separation of the e–h pairs, which are spatially separated on the Fe and Cr sites [34]. Transition metals (TM), in particular Mn-doped BFO, have also been investigated and have been demonstrated to improve the photoferroic properties of BFO [35].

Besides BFO-based materials, other possible photoferroic materials with appropriate band gaps include $KBiFe_2O_5$ [40], $[KNbO_3]_{1-x}[BaNi_{0.5}Nb_{0.5}O_{3-\delta}]_x$ [41], $BiFe_{1-x}Co_xO_3$ [43], Bi_2ZnTiO_6, [44] hexagonal ferrite (h-$RFeO_3$, R = Y, Dy–Lu) thin films [45], Ni-doped $SrBi_2Nb_2O_9$ [46], and composite thin films of mixed $BiMnO_3$ and $BiMn_2O_5$ [47].

Besides oxide single-phase or its composites, an alternative way to design photoferroic materials is to combine ferroelectric oxides with good light-absorbing semiconductors in a multilayer heterostructure, where the semiconductor absorbs photons and generates the e–h pairs, and the conventional ferroelectric oxide provides the driving forces to separate the e–h pairs [48–51]. Some of the most promising photoferroics and the typical performances of their single-layer ferroelectric thin-film solar cells are listed in table 1. Almost all of the substituted single-phase systems end up with either too large a band gap or too little polarization, and the power conversion efficiency remains low. Moreover, oxide perovskites containing 3d transition metal cations typically have heavy carrier effective masses due to the non-dispersive band edges derived from the localized 3d orbitals. This results in low mobility and high recombination rates of the carriers [52]. Currently, it still remains unclear whether there is an intrinsic limit to the power conversion efficiency of the hitherto-investigated ferroelectric photoabsorbers. On the other hand, several Bi-based double oxoperovskites have shown both narrow band gaps and large charge mobility as well as small exciton binding energies. $Ba_2Bi^{3+}Bi^{5+}O_6$ and $Ba_2Bi^{3+}(Bi^{5+}_{0.4}Nb^{5+}_{0.6})O_6$, for example, have band gaps of 2.1 eV and 1.6 eV, respectively [53]. These oxide double perovskites have also

shown high performance as photocatalysts for water oxidation [54]. Chalcogenide perovskites have recently been predicted to exhibit narrow band gaps as well as reasonably small carrier effective masses. Ruddlesden–Popper (RP) perovskite sulfides ($A_3B_2S_7$) could be a new family of ferroelectric photovoltaic materials with large photoabsorption of solar light [55], as we describe in the next section. However, it is still a challenge to make high-quality sulfide thin films with negligible deep defect states. It has been shown that the large amount of defects and disorder in the bulk structure of the sulfide light-harvesting layer limits the minority charge carrier lifetimes and enhances recombination processes [56].

3. *In silico* discovery of photoferroic materials

The discovery of novel materials using quantum mechanical simulations is a possible way to overcome the challenges described above. In the last few decades, there have been multiple studies on *in silico* design of novel materials for PV devices as well as new ferroelectrics. Recent examples include novel light-harvesting materials based on inorganic and metal–organic perovskites, oxynitride and sulfide materials, and known materials from existing databases [20–23, 57–64]. In the case of ferroelectrics there has recently been some progress in obtaining design rules that can readily be applied to computational discovery of new materials exhibiting switchable spontaneous polarization. In particular, for improper ferroelectric perovskites, spontaneous polarization typically arises from tilts or rotations of the BO_6 octahedra [65–67] and it has been shown that polar materials can be constructed from inversion-symmetric parent compounds by substituting atoms that eliminate inversion centers and conserve certain pseudo-inversion centers [25].

The combination of optimized absorption properties and ferroelectric order at room temperature define a new route towards the discovery of novel photoferroic materials. In [68], it was shown that the band gap of the ferroelectric $KNbO_3$ could be reduced to the frequency range of visible light by Zn or Bi substitution. Three naturally occurring materials (enargite, stephanite, and bournonite) have recently been suggested as possible candidates from a pool of around 200 materials using criteria based on band gap, optical response, effective masses, and spontaneous polarization [69]. Similar criteria have been applied to polar and non-polar chalcogenide perovskites in the layered RP phase [55, 70]; $Ca_3Z_2S_7$, $Ca_3Hf_2S_7$, $Ca_3Zr_2Se_7$, and $Ca_3Hf_2S_7$ have good band gaps for PV systems and are stable in a ferroelectric phase with non-trivial polarization. The role of the Goldschmidt tolerance factor [71] as a design rule for ferroelectric RP materials has been discussed. Combining V and Fe in a double perovskite gives rise to a non-zero polarization because of charge transfer from V to Fe, which generates empty V-d orbitals and half-filled Fe-d orbitals. The V-d^0 configuration also has the effect of reducing the band gap compared to AVO_3 and $AFeO_3$ perovskites, making combinations like Ba_2VFeO_6 possible candidates for photoferroic devices [72].

3.1. High-throughput approach and identification of descriptors

The materials mentioned above have been identified using high-throughput approaches guided by a screening funnel (figure 2). Starting with a large number of possible configurations, at each step of the funnel the computational cost and complexity increases and materials that do not fulfill the required criteria are removed from the pool of possible candidates. The definition of the link (descriptors) between the macroscopic properties required by the device, the selection criteria, and the microscopic quantities calculated with the simulations is a requirement for any high-throughput screening study [16]. In the following, we describe the most important descriptors and criteria for identifying novel photoferroic materials.

3.1.1. Chemical intuition

Data-mining experimental and computational databases are one of the possible starting points for a screening study. This provides information on possible interesting crystal structures to use for templates, or on the chemical elements that have produced interesting materials for the target application. Chemical intuition as well as structural and chemical rules [73, 74], such as counting the number of electrons and the tolerance factor, can reduce the number of possible combinations to calculate.

3.1.2. Stability

Stability against phase change and segregation in different materials is a requirement for any novel material. The stability can be calculated by comparing the energy of the candidate materials with the energies of the possible competing phases, which are taken from theoretical and experimental databases, like the Materials Project [75], Open Quantum Materials Database (OQMD) [76], or Inorganic Crystal Structure Database (ICSD) [77]. At a given composition it is thus possible to identify which structure has the lowest energy, i.e. is stable at 0 K. However, there might be synthesis methods or conditions that allow metastable materials to be synthesized [78, 79]. To take this into account, the stability criterion could be relaxed to include a slight metastability (the

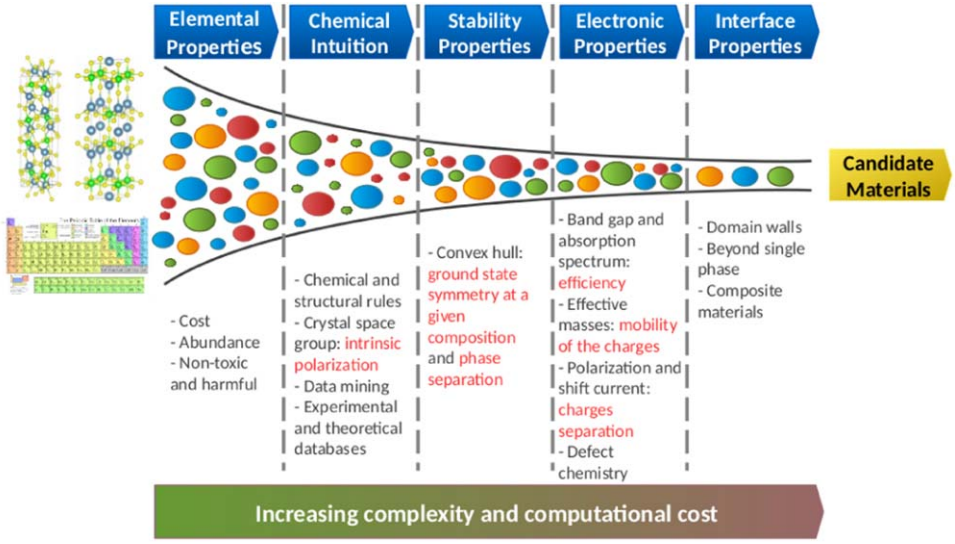

Figure 2. Funnel and required properties for novel photoferroic materials.

candidate could be considered metastable if their energy is up to 0.2 eV/atom higher than the ground state combination) [20].

3.1.3. Spontaneous polarization

Photoferroic materials rely on ferroelectricity, so materials that are not ferroelectric because of their centrosymmetry could be discarded from the funnel before calculating the electronic properties. Ferroelectric materials are characterized by having a finite electric polarization that can be switched by an external electric field. Such switching involves a structural deformation that connects degenerate ground states with different polarization and a particular ground state will thus have a spontaneously broken symmetry. However, the spontaneous polarization is not well defined for bulk materials, since the integrated dipole density will depend on the choice of unit cell. Polarization changes, on the other hand, are well defined and can be calculated from the polarization current induced by an adiabatic structural deformation. This approach leads to the Berry phase formula [90, 91], which provides a formal expression for the polarization in an atomic configuration parameterized by λ:

$$\mathbf{P}(\lambda) = \frac{e}{(2\pi)^2} Im \sum_{occ} \int_{BZ} d^3k \langle u_{n\mathbf{k}} | \nabla_{\mathrm{k}} | u_{n\mathbf{k}} \rangle + \frac{e}{V} \sum_a Z_a \mathbf{R}_a \,. \quad (1)$$

Here e is the charge of the electron, u_{nk} are the periodic parts of the Bloch states and R_a is the position of an atom with nuclear charge Z_a. The Berry phase formula can thus be used to calculate changes in polarization under structural deformations and the spontaneous polarization can be defined as the polarization relative to a non-ferroelectric structural phase. Equation (1) has been applied to predict the spontaneous polarization of a wide range of ferroelectrics and yield reasonable agreement with experimental values [92], although the results can be somewhat dependent on the choice of exchange–correlation functional [81]. Moreover, the expression provides an easy way to calculate the Born effective charges [93], which determine the atomic displacements under an applied electric field and account for the splitting of longitudinal optical phonons at the Brillouin zone center [94]. A selection of ferroelectric materials with calculated polarization and band gaps is displayed in table 2.

3.1.4. Electronic properties

Once the (meta)stable ferroelectric candidates have been identified, the funnel proceeds with the calculation of the electronic properties. The band gaps (table 2) obtained from the Kohn–Sham spectrum in DFT are typically significantly smaller than the experimental values. For example, $PbTiO_3$ could appear suitable for light-harvesting with a gap of ~1.5 eV, but the experimental gap is more than a factor of two larger, which indicates that it can only absorb a rather small fraction of solar light. The computational discovery of novel photoferroics thus crucially depends on accurate estimates of the band gaps and cannot solely be based on the prediction of local/semi-local functionals like local-density approximations (LDA) or Perdew–Burke–Ernzerhof (PBE). The self-interaction error for semi-local exchange–correlation functionals [95] and the missing derivative discontinuity [96] are mainly responsible for the underestimation of the band gap. Hybrid functionals, which include a fraction of exact exchange, for example HSE06 [97]; many-body methods, like the GW approximation

Table 2. Calculated band gap and spontaneous polarization of selected ferroelectric perovskites.

Material	Crystal symmetry	E_g [eV]	P [μC cm^{-2}]	DFT xc-functional	References
$BaTiO_3$	Tetragonal, P4mm	1.92	26	LDA	[80, 81]
$BaTiO_3$	Tetragonal, P4mm	1.84	48	PBE	[80, 81]
$BaTiO_3$	Tetragonal, P4mm		35	PBEsol	[81]
$PbTiO_3$	Tetragonal, P4mm	1.40	78	LDA	[80, 81]
$PbTiO_3$	Tetragonal, P4mm	1.56	128	PBE	[80, 81]
$PbTiO_3$	Tetragonal, P4mm		98	PBEsol	[81]
$KNbO_3$	Tetragonal, P4mm		27	LDA	[81]
$KNbO_3$	Tetragonal, P4mm	1.48	51	PBE	[81, 82]
$KNbO_3$	Tetragonal, P4mm		38	PBEsol	[81]
$BiFeO_3$	Rhombohedral, R3c	0.4	98.7	LDA	[83]
$BiFeO_3$	Rhombohedral, R3c	1.9	93.3	LDA+U	[83]
$TbMnO_3$	Orthorhombic, Pbnm	0.5	−0.47	LDA+U	[84]
$YMnO_3$	Hexagonal, $P6_3cm$	0.45–0.9	6.5	LDA+U	[85–87]
$SrBi_2Ta_2O_9$	Orthorhombic, $A2_1am$	2.28	23.8	PBE	[88, 89]
$Ca_3Zr_2Se_7$	Orthorhombic, $Cmc2_1$	1.8	∼16	HSE06	[70]
$Ca_3Hf_2Se_7$	Orthorhombic, $Cmc2_1$	2.1	∼14	HSE06	[70]
$Ca_3Zr_2S_7$	Orthorhombic, $Cmc2_1$	2.3	∼16	HSE06	[70]
$Ca_3Hf_2S_7$	Orthorhombic, $Cmc2_1$	2.6	∼14	HSE06	[70]

[98]; and exchange–correlation functionals, which explicitly include the calculation of the derivative discontinuity, such as the GLLB-SC functional [99], are possible solutions to the underestimation of the band gap. The latter, in particular, have been extensively used to identify light-harvesting materials using a high-throughput approach because of its computational cost, which is comparable with a standard DFT calculation, and accuracy, which is similar to the hybrid and many-body methods [59]. Although the band gap is the simplest descriptor for the efficiency of a light-harvesting device, it gives no information on the character or strength of the transition, which ultimately determine the efficiency. More accurate descriptors that take these points into consideration can be obtained by combining the character of the gap with the shape of the absorption at the band gap edges and the non-radiative recombination losses (spectroscopic limited maximum efficiency (SLME) metric) [100], or calculating the absorption spectrum by means of time-dependent DFT and convolving it with the solar spectrum [61]. Band structures and effective masses can provide useful information as descriptors to the mobility of the e–h pairs generated by the absorbed photons. The presence of defects might induce mid-gap states in the band gap. Recently a descriptor based on the character of the valence and conduction bands, to estimate whether a material is defect tolerant or sensitive, has been established [101].

3.1.5. Shift current

The bulk photovoltaic effect denotes the ability of a material to sustain a DC current (J) in response to an AC electric field (E). This is the mechanism underlying the photovoltaic response in photoferroics, and a quantitative measure of the ability to separate photoexcited e–h pairs by intrinsic electric fields in ferroelectrics is provided by the shift current

$$J_i = \sum_{jk} \sigma_{ijk}(\omega) E_j(\omega) E_k(-\omega), \tag{2}$$

where the subscripts indicate the spatial components of the current and field. Clearly, the effect originates from a non-linear response, since the linear response can only give rise to currents oscillating at the same frequency as the perturbing field. Quantitatively the effect is encompassed by the second-order conductivity σ_{ijk}. Since the current as well as the electric field changes sign under space inversion, the second-order conductivity must vanish in materials with inversion symmetry. Moreover, non-polar materials with inversion symmetry can only sustain a finite shift current under coherent (polarized) illumination and are therefore irrelevant for applications relying on solar light. First-principles calculations have established that the shift current accurately accounts for the photocurrent observed in $BaTiO_3$ [102] and thus seems to comprise the main mechanism underlying the bulk photovoltaic effect. Since the shift current mechanism does not rely on a built-in electric field, the photovoltage is not limited by the band gap. The efficiency of photovoltaics based on the bulk photovoltaic effect is thus not limited by the SQ limit and provides an intriguing alternative that may beat the performance of traditional photovoltaics if the right material is discovered. In [50], the conditions for a large non-linear current response were analyzed. Essentially, the response has a structure similar to a linear response, except that the dipole transition matrix elements are weighted by a k-point and band-dependent shift vector. It is thus desirable to have a large joint density of state at the band edges as well as large dipole matrix elements. However, for ferroelectrics the shift vector is not always simply correlated with the spontaneous polarization, and the shift

currents in $BaTiO_3$ and $PbTiO_3$ have similar magnitude despite the fact that the polarization in $PbTiO_3$ is more than twice the value of that in $BaTiO_3$. In contrast, the shift current in monolayers of Ge and Sn chalcogenides has been shown to be directly proportional to the spontaneous polarization [103]. The theoretical prediction of efficient photovoltaics based on the bulk photovoltaic effect thus remains a major challenge and requires full first-principles calculations for a given candidate material. A general *ab-initio* scheme for calculating the shift current was recently implemented in Wannier90 [104], which is interfaced to several electronic structure codes. It is thus straightforward to calculate the shift current in a given material and it seems plausible that high-throughput calculations could be based on such an approach.

3.1.6. Role of domain walls

Ferroelectric materials under ambient conditions typically exhibit polarization domains, i.e. regions of uniform polarization. The boundaries between domains are known as domain walls and are characterized by a discontinuity in the polarization vectors of adjacent domains. Domain walls thus give rise to local electric fields that may strongly influence the physical properties of ferroelectrics. In general it is expected that domain walls are detrimental to transport properties since they provide regions of strong scattering. However, it has been demonstrated that domain walls provide a significant contribution to the photovoltaic properties of $BiFeO_3$ [105] and for Mn-doped $BaTiO_3$ the bulk photovoltaic effect was reported to increase by orders of magnitude due to domain walls [106]. A similar effect has been demonstrated for thin films of $BaTiO_3$ [107]. The reason is likely to be related to the fact that domain walls or surfaces may provide local electric fields that help separate (first-order) photoexcited carriers similar to the dominating mechanism in traditional p–n photovoltaics. The significance of this effect in photoferroics is still poorly understood and subject to some debate, but for the purpose of comparing calculated photocurrents with experiments, it will be crucial to separate the effect of domain walls and surfaces. This can be done either by comparing shift current calculations to experiments on single-domain ferroelectrics, or preferably, to develop a theoretical framework that quantitatively takes the effect of domain walls and surfaces into account. The latter approach could also give rise to new design principles for optimized photoferroics based on domain wall/device architecture.

3.1.7. Screening criteria

The necessary, basic criteria for a material to be used in a PV device can be summarized as: stability (heat of formation $\leqslant$ 0.2 eV/atom), efficient harvest of visible light (1.0 $\leqslant$ band gap $\leqslant$ 2.0 eV, to account for small inaccuracies in the calculations), and good mobility of the photogenerated charges (small effective masses). These criteria also apply to photoferroic materials, but in this case the presence of spontaneous polarization and non-linear photoconductivity comprise additional crucial descriptors for the performance of photoferroic PV devices (the calculation of the shift currents is still too expensive to be used as a descriptor in a screening fashion). These criteria can be applied to various search spaces, in terms of both which chemical elements and which crystal structure templates to use. From an academic point of view, the selection of chemical elements should be as broad as possible to avoid ruling out any possible interesting combination. However some chemicals might need to be excluded during the experimental synthesis and device preparation based on considerations such as abundance, toxicity, cost, weight, etc. Optimal templates for screening projects are structures that can accommodate multiple chemicals and are not too computationally expensive, i.e. do not contain too many atoms in the unit cell. Some examples are binary structures, like rock salt and wurtzite, ternary structures, like perovskite, or 2D materials, like transition metal dichalcogenides. A detailed description of a high-throughput approach for the discovery of light-harvesting materials can be found elsewhere in the literature [108].

We would like to note that different methods have been proposed to estimate the efficiency of a PV device based on photoferroic materials [9, 50, 105]. Despite this, the maximum theoretical efficiency for emerging photoferroic materials is rarely available from the literature, due among other reasons to the complexity of the required calculations as well as of all the possible losses. In most cases, a rough estimation of the efficiency can be given by the band gap and the presence of an intrinsic polarization.

4. Outlook

Single-phase photoferroic materials remain rare. The discovery of new ferroelectric materials with band gaps approaching the ideal value of 1.34 eV, corresponding to the maximum efficiency for a single p−n junction PV [109], definitely represents an important milestone in photoferroelectrics. Additionally, enhanced photoresponse under visible light of a typical wide-gap ferroelectric material has been achieved by combining it with a semiconductor material with a narrow band gap, but the efficiency remains below 1.5% [110]. So far, the majority of the work has focused on band gap engineering of the photoabsorber layer, and the carrier mobility remains under-investigated. Besides single-phase and composites, double perovskite ferroelectrics with good

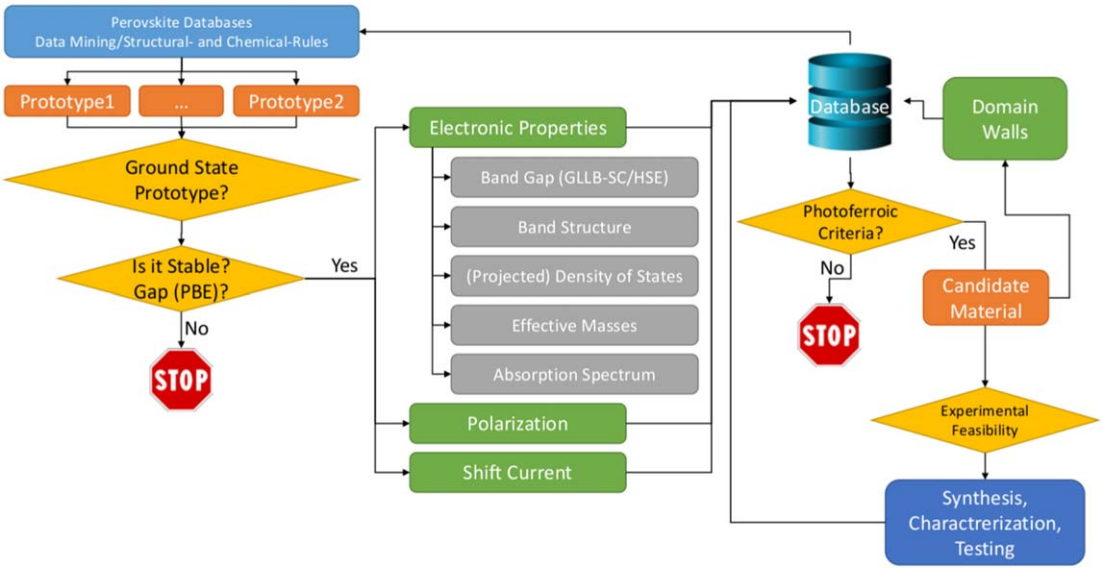

Figure 3. Example of a workflow for the computational discovery of novel photoferroic materials.

charge mobility [72] can be achieved by layer-by-layer atomically engineered epitaxial oxide interfaces [111], and appear highly promising. Furthermore, optimization of the interfaces or electrode/photoabsorber connections for ferroelectric PV cells remains rare. In particular, a Schottky barrier could be formed at the metal–ferroelectric interface of a metal–ferroelectric–metal trilayer solar cell, and the built-in field in the depletion region could largely influence the carrier mobility and may even provide a driving force for the PV effect as in the typical junction-based solar cells. Therefore, new strategies should be set up to optimize cell efficiency based on photoferroic materials. Additionally, potential improvements in photovoltaic efficiency would also result in greater photocatalytic and photoelectrochemical activity, opening new paths to light energy conversion beyond photovoltaic solar cells. In a photoelectrocatalytic device (PEC), water is dissociated into oxygen and hydrogen molecules by means of solar light (figure 1(c)). This technology is based on similar criteria to a PV device plus stability in a water environment which can be addressed using Pourbaix diagrams [112, 113]. The criterion of the band gap, in addition, should take into account that the bare energy to split water is 1.23 eV per molecule, and losses like overpotentials associated with the hydrogen and oxygen evolution processes (around 0.1 and 0.4 eV, respectively [114]) and the non-equilibrium condition of the photogenerated electrons and holes has the effect of splitting the Fermi level into electron and hole quasi-Fermi levels (loss of about 0.25 eV for each band edge) [115]. The required band gap should thus be of the order of 2.2 eV, much larger than the required gap for optimal PV materials. The main advantage of PEC over PV is that solar energy is converted into chemical energy (H_2 and O_2), which is easier to store than the electricity produced by PV devices. Detailed analysis of the feasibility and challenges of PEC devices can be found in the literature [1, 116]. The use of photoferroic materials for PEC can improve the efficiency of these devices, by generating large photovoltages that can more easily provide the required energy to overcome all the losses and overpotentials, while still harvesting a significant fraction of the solar energy. Experiments have already pioneered the use of photoferroics in PEC devices, as highlighted in a recent review [117]. It has been shown, for example, that the separation of charges can be enhanced in materials like $PbTiO_3$ thanks to their intrinsic ferroelectricity [118, 119]. However, most of the materials investigated have a band gap close to the UV part of the spectrum and thus absorb only a small fraction of solar energy. The unique combination of ferroelectric and optical properties opens the door to the development of multisource energy harvesting or multifunctional sensing devices for the simultaneous and efficient conversion of solar, thermal, and kinetic energies into electricity in a single material [120].

All these possible applications require fast discovery of novel materials. Workflows are designed to automate this process and to assure provenance and standardization of the data. Starting from a pool of possible interesting materials, each step of the workflow takes care of a well defined calculation or decision, which is connected with previous and subsequent steps. As shown in figure 3, the candidate materials can be selected from existing databases or using data-mining tools. Different polymorphs or prototypes of the given composition are calculated to identify the ground state structure. Some of these templates are non-polar and thus will not support ferroelectricity, and the combination can therefore be discarded. It is important to note that metastable polymorphs can also be of interest and should not be removed from the pool of candidate materials. It has been shown that metastable compounds with energy of around 100 meV/atom above the

ground state can be synthesized and stable at appropriate external conditions [78]. Once the ground state is identified, we proceed to calculate the stability against phase separation and the band gap using standard DFT methods at the generalized gradient approximation (GGA) level [121]. If the candidate material is (meta)stable and shows a band gap, one proceeds with calculating the electronic properties at a more accurate level as well as polarization and shift current. These data are collected in a database, which will contribute to the selection of the next materials to calculate. Selection criteria will be applied to the candidate materials. If a material fulfills these criteria, it is possible to proceed with an analysis of the experimental feasibility (elemental cost, abundance, toxicity, possible synthesis routes, etc.) and eventually with synthesis and characterization, which will be included in the database to provide experimental verification. More accurate calculations, for example to understand the role of domain walls, can be performed at this point. Artificial intelligence and machine learning can be helpful in accelerating the discovery of materials, although that discussion is beyond the scope of this paper. It is important to note that most of the available workflows are computational and only a few have been developed to cover the full material discovery from simulations to experiments, especially in connection with organic synthesis and testing [122]. The complexity of synthesis for new materials is, in many cases, still a matter of experience and proceeds in a trial-and-error way. A close synergy between experiments and theory, as well as the development of theoretical tools to predict the most promising synthesis path, is one of the ways to solve this issue.

Acknowledgments

IEC acknowledges support from the Department of Energy Conversion and Storage, Technical University of Denmark, through the Special Competence Initiative 'Autonomous Materials Discovery (AiMade)' [123]. YZC acknowledges the financial support from the European Union's H2020-FETPROACT Grant No. 824072, the support from Agency for Science and Higher Education of Denmark, Grant No. 8073-00014B, and the Independent Research Fund Denmark, Grant No. 9041-00034B.

ORCID iDs

Ivano E Castelli https://orcid.org/0000-0001-5880-5045
Thomas Olsen https://orcid.org/0000-0001-6256-9284
Yunzhong Chen https://orcid.org/0000-0001-8368-5823

References

[1] Sivula K and van de Krol R 2016 *Nature Rev. Mater.* **1** 15010
[2] Shockley W and Queisser H J 1961 *J. Appl. Phys.* **32** 510–9
[3] Nayak P K, Mahesh S, Snaith H J and Cahen D 2019 *Nature Rev. Mater.* **4** 269–85
[4] NREL Best Research-Cell Efficiency Chart (https://nrel.gov/pv/cell-efficiency.html)
[5] Chiarella F, Zappettini A, Licci F, Borriello I, Cantele G, Ninno D, Cassinese A and Vaglio R 2008 *Phys. Rev.* B **77** 045129
[6] EPA United States Environmental Protection Agency (https://epa.gov/lead)
[7] Butler K T, Frost J M and Walsh A 2015 *Energy & Environ. Sci.* **8** 838–48
[8] Mehta R R 1972 *Ferroelectrics* **4** 5–18
[9] Lopez-Varo P *et al* 2016 *Phys. Rep.* **653** 1–40
[10] Wong L H, Zakutayev A, Major J D, Hao X, Walsh A, Todorov T K and Saucedo E 2019 *J. Phys.: Energy* **1** 032001
[11] Hohenberg P and Kohn W 1964 *Phys. Rev.* **136** 864
[12] Kohn W and Sham L J 1965 *Phys. Rev.* **140** 1133
[13] Haastrup S *et al* 2018 *2D Mater.* **5** 042002
[14] Olsen T, Andersen E, Okugawa T, Torelli D, Deilmann T and Thygesen K S 2019 *Phys. Rev. Mater.* **3** 024005
[15] Torelli D, Thygesen K S and Olsen T 2019 *2D Mater.* **4** 045018
[16] Curtarolo S, Hart G L W, Nardelli M B, Mingo N, Sanvito S and Levy O 2013 *Nat. Mater.* **12** 191–201
[17] Marzari N 2016 *Nat. Mater.* **15** 381–2
[18] Seminario J (ed) 1996 *Recent Developments and Applications of Modern Density Functional Theory* (*Theoretical and Computational Chemistry*) (Amsterdam: Elsevier)
[19] Lejaeghere K *et al* 2016 *Science* **351** 1415
[20] Castelli I E, Olsen T, Datta S, Landis D D, Dahl S, Thygesen K S and Jacobsen K W 2012 *Energy & Environ. Sci.* **5** 5814–9
[21] Castelli I E, Landis D D, Thygesen K S, Dahl S, Chorkendorff I, Jaramillo T F and Jacobsen K W 2012 *Energy & Environ. Sci.* **5** 9034
[22] Wu Y, Lazic P, Hautier G, Persson K and Ceder G 2013 *Energy & Environ. Sci.* **6** 157–68
[23] Kuhar K, Crovetto A, Pandey M, Thygesen K S, Seger B, Vesborg P C K, Hansen O, Chorkendorff I and Jacobsen K W 2017 *Energy & Environ. Sci.* **10** 2579–93
[24] Scott J F 2015 *NPJ Comput. Mater.* **1** 15006
[25] Xu K, Lu X Z and Xiang H 2017 *NPJ Quantum Mater.* **2** 1
[26] Ishihara T 2009 *Perovskite Oxide for Solid Oxide Fuel Cells* (Berlin: Springer)
[27] Fridkin V M 1980 *Ferroelectric Semiconductors* (Berlin: Springer)
[28] Fong C, Petroff Y, Kohn S and Shen Y 1974 *Solid State Commun.* **14** 681–5

[29] Nie R, Sung Y H, Paik M J, Mehta A, Wook P B, Choi Y C and Seok S I 2017 *Adv. Energy Mater.* **8** 1701901
[30] Yuan Y, Xiao Z, Yang B and Huang J 2014 *J. Mater. Chem.* A **2** 6027–41
[31] Song S, Kim D, Jang H M, Yeo B C, Han S S, Kim C S and Scott J F 2017 *Chem. Mater.* **29** 7596–603
[32] Choi T, Lee S, Choi Y J, Kiryukhin V and Cheong S W 2009 *Science* **324** 63–6
[33] Nechache R, Harnagea C, Li S, Cardenas L, Huang W, Chakrabartty J and Rosei F 2014 *Nat. Photonics* **9** 61–7
[34] Kim D, Han H, Lee J H, Choi J W, Grossman J C, Jang H M and Kim D 2018 *Proc. Natl Acad. Sci.* **115** 6566–71
[35] Matsuo H, Noguchi Y and Miyayama M 2017 *Nat. Commun.* **8** 207
[36] Dharmadhikari V S and Grannemann W W 1982 *J. Appl. Phys.* **53** 8988–92
[37] Dubovik E, Fridkin V and Dimos D 1995 *Integr. Ferroelectr.* **8** 285–90
[38] Glass A M, von der Linde D and Negran T J 1974 *Appl. Phys. Lett.* **25** 233–5
[39] Yang S Y *et al* 2009 *Appl. Phys. Lett.* **95** 062909
[40] Zhang G, Wu H, Li G, Huang Q, Yang C, Huang F, Liao F and Lin J 2013 *Sci. Rep.* **3** 1265
[41] Grinberg I *et al* 2013 *Nature* **503** 509–12
[42] Chakrabartty J P, Nechache R, Harnagea C and Rosei F 2013 *Opt. Express* **22** A80
[43] Machado P *et al* 2019 *Chem. Mater.* **31** 947–54
[44] Figueiras F G *et al* 2019 *J. Mater. Chem.* A **7** 10696–701
[45] Han H, Kim D, Chae S, Park J, Nam S Y, Choi M, Yong K, Kim H J, Son J and Jang H M 2018 *Nanoscale* **10** 13261–9
[46] Wu M, Lou X, Li T, Li J, Wang S, Li W, Peng B and Gou G 2017 *J. Alloys Compd.* **724** 1093–100
[47] Chakrabartty J, Harnagea C, Celikin M, Rosei F and Nechache R 2018 *Nat. Photonics* **12** 271–6
[48] Cao D, Wang C, Zheng F, Dong W, Fang L and Shen M 2012 *Nano Lett.* **12** 2803–9
[49] Fan Z, Yao K and Wang J 2014 *Appl. Phys. Lett.* **105** 162903
[50] Tan L Z, Zheng F, Young S M, Wang F, Liu S and Rappe A M 2016 *NPJ Comput. Mater.* **2** 16026
[51] Silva J, Sekhar K, Cortés-Juan F, Negrea R, Kuncser A, Connolly J, Ghica C and Moreira J A 2018 *Sol. Energy* **167** 18–23
[52] Wang L, Ma H, Chang L, Ma C, Yuan G, Wang J and Wu T 2016 *Small* **13** 1602355
[53] Tang J, Zou Z and Ye J 2007 *J Phys. Chem.* C **111** 12779–85
[54] Weng B, Xiao Z, Meng W, Grice C R, Poudel T, Deng X and Yan Y 2016 *Adv. Energy Mater.* **7** 1602260
[55] Wang H, Gou G and Li J 2016 *Nano Energy* **22** 507–13
[56] Wallace S K, Mitzi D B and Walsh A 2017 *ACS Energy Lett.* **2** 776–9
[57] Castelli I E, Garcia-Lastra J M, Hüser F, Thygesen K S and Jacobsen K W 2013 *New J. Phys.* **15** 105026
[58] Castelli I E, Thygesen K S and Jacobsen K W 2013 *MRS Proceedings* **vol 1523** (Cambridge: Cambridge University Press) Mrsf12-1523-qq07-06
[59] Castelli I E, Hüser F, Pandey M, Li H, Thygesen K S, Seger B, Jain A, Persson K A, Ceder G and Jacobsen K W 2014 *Adv. Energy Mater.* **5** 1400915
[60] Castelli I E, García-Lastra J M, Thygesen K S and Jacobsen K W 2014 *APL Mater.* **2** 081514
[61] Castelli I E, Thygesen K S and Jacobsen K W 2015 *J. Mater. Chem.* A **3** 12343–9
[62] Pilania G, Mannodi-Kanakkithodi A, Uberuaga B P, Ramprasad R, Gubernatis J E and Lookman T 2016 *Sci. Rep.* **6** 19375
[63] Kuhar K, Pandey M, Thygesen K S and Jacobsen K W 2018 *ACS Energy Lett.* **3** 436–46
[64] Agiorgousis M L, Sun Y Y, Choe D H, West D and Zhang S 2019 *Adv. Theory and Simulations* **2** 1800173
[65] Rondinelli J M and Fennie C J 2012 *Adv. Mater.* **24** 1918–1918
[66] Young J and Rondinelli J M 2013 *Chem. Mater.* **25** 4545–50
[67] Benedek N A, Rondinelli J M, Djani H, Ghosez P and Lightfoot P 2015 *Dalton Trans.* **44** 10543–58
[68] Wang F, Grinberg I, Jiang L, Young S M, Davies P K and Rappe A M 2015 *Ferroelectrics* **483** 1–12
[69] Wallace S K, Svane K L, Huhn W P, Zhu T, Mitzi D B, Blum V and Walsh A 2017 *Sustainable Energy & Fuels* **1** 1339–50
[70] Zhang Y, Shimada T, Kitamura T and Wang J 2017 *J. Phys. Chem. Lett.* **8** 5834–9
[71] Goldschmidt V M 1926 *Naturwissenschaften* **14** 477–85
[72] Chen H and Millis A 2017 *Sci. Rep.* **7** 6142
[73] Jain A, Castelli I E, Hautier G, Bailey D H and Jacobsen K W 2013 *J. Mater. Sci.* **48** 6519–34
[74] Castelli I E and Jacobsen K W 2014 *Modell. Simul. Mater. Sci. Eng.* **22** 055007
[75] Materials Project—A Materials Genome Approach (http://materialsproject.org/)
[76] The Open Quantum Materials Database (http://oqmd.org/)
[77] ICSDWeb (http://fiz-karlsruhe.de/icsd_web.html)
[78] Sun W, Dacek S T, Ong S P, Hautier G, Jain A, Richards W D, Gamst A C, Persson K A and Ceder G 2016 *Sci. Adv.* **2** e1600225
[79] Aykol M, Dwaraknath S S, Sun W and Persson K A 2018 *Scie. Adv.* **4** eaaq0148
[80] Piskunov S, Heifets E, Eglitis R and Borstel G 2004 *Comput. Mater. Sci.* **29** 165–78
[81] Yuk S F, Pitike K C, Nakhmanson S M, Eisenbach M, Li Y W and Cooper V R 2017 *Sci. Rep.* **7** 43482
[82] Faridi M, Tariq S, Jamil M I, Batool A, Nadeem S and Amin A 2018 *Chin. J. Phys.* **56** 1481–7
[83] Neaton J B, Ederer C, Waghmare U V, Spaldin N A and Rabe K M 2005 *Phys. Rev.* B **71** 014113
[84] Malashevich A and Vanderbilt D 2008 *Phys. Rev. Lett.* **101** 037210
[85] Biswas T and Jain M 2016 *J. Appl. Phys.* **120** 155102
[86] Qian M, Dong J and Xing D Y 2001 *Phys. Rev.* B **63** 155101
[87] Fennie C J and Rabe K M 2005 *Phys. Rev.* B **72** 100103
[88] Zhao N, Wang Y H, Zhao X Y, Zhang M and Gong S 2011 *Chin. Phys. Lett.* **28** 077101
[89] Ke H, Wang W, Zheng Z, Tang C, Jia D, Lu Z and Zhou Y 2010 *J. Phys. Condens. Matter* **23** 015901
[90] hua Xu J and Freeman A J 1993 *Phys. Rev.* B **47** 165–73
[91] Vanderbilt D and King-Smith R D 1993 *Phys. Rev.* B **48** 4442–55
[92] Resta R and Vanderbilt D 2007 Theory of polarization: a modern approach *Physics of Ferroelectrics* (*Topics in Applied Physics* vol 105) (Berlin: Springer) pp 31–68
[93] Marzari N and Vanderbilt D 1998 *Maximally-Localized Wannier Functions in Perovskites: Cubic $BaTiO_3$* (New York: AIP)
[94] Gonze X and Lee C 1997 *Phys. Rev.* B **55** 10355–68
[95] Perdew J P and Zunger A 1981 *Phys. Rev.* B **23** 5048–79
[96] Godby R W, Schlüter M and Sham L J 1986 *Phys. Rev. Lett.* **56** 2415–8
[97] Heyd J, Scuseria G E and Ernzerhof M 2003 *J. Chem. Phys.* **118** 8207–15
[98] Aryasetiawan F and Gunnarsson O 1998 *Rep. Prog. Phys.* **61** 237–312

[99] Kuisma M, Ojanen J, Enkovaara J and Rantala T T 2010 *Phys. Rev.* B **82** 115106
[100] Yu L and Zunger A 2012 *Phys. Rev. Lett.* **108** 068701
[101] Zakutayev A, Caskey C M, Fioretti A N, Ginley D S, Vidal J, Stevanović V, Tea E and Lany S 2014 *J. Phys. Chem. Lett.* **5** 1117–25
[102] Young S M and Rappe A M 2012 *Phys. Rev. Lett.* **109** 116601
[103] Rangel T, Fregoso B M, Mendoza B S, Morimoto T, Moore J E and Neaton J B 2017 *Phys. Rev. Lett.* **119** 067402
[104] Ibañez-Azpiroz J, Tsirkin S S and Souza I 2018 *Phys. Rev.* B **97** 245143
[105] Matsuo H, Kitanaka Y, Inoue R, Noguchi Y, Miyayama M, Kiguchi T and Konno T J 2016 *Phys. Rev.* B **94** 214111
[106] Inoue R, Ishikawa S, Imura R, Kitanaka Y, Oguchi T, Noguchi Y and Miyayama M 2015 *Sci. Rep.* **5** 14741
[107] Zenkevich A, Matveyev Y, Maksimova K, Gaynutdinov R, Tolstikhina A and Fridkin V 2014 *Phys. Rev.* B **90** 161409
[108] Castelli I E, Kuhar K, Pandey M and Jacobsen K W 2018 Computational screening of light-absorbing materials for photoelectrochemical water splitting *Advances in Photoelectrochemical Water Splitting: Theory, Experiment and Systems Analysis* (Cambridge: Royal Society of Chemistry) pp 62–99
[109] Rühle S 2016 *Sol. Energy* **130** 139–47
[110] Zheng F *et al* 2014 *J. Mater. Chem.* A **2** 1363–8
[111] Chen Y Z *et al* 2015 *Nat. Mater.* **14** 801–6
[112] Persson K A, Waldwick B, Lazic P and Ceder G 2012 *Phys. Rev.* B **85** 235438
[113] Castelli I E, Thygesen K S and Jacobsen K W 2013 *Top. Catal.* **57** 265–72
[114] Suffredini H 2000 *Int. J. Hydrogen Energy* **25** 415–23
[115] van de Krol R and Grätzel M (ed) 2012 *Photoelectrochemical Hydrogen Production* (New York: Springer)
[116] Roger I, Shipman M A and Symes M D 2017 *Nature Rev. Chem.* **1** 0003
[117] Kim S, Nguyen N and Bark C 2018 *Appl. Sci.* **8** 1526
[118] Li R, Zhao Y and Li C 2017 *Faraday Discuss.* **198** 463–72
[119] Zhen C, Yu J C, Liu G and Cheng H M 2014 *Chem. Commun.* **50** 10416
[120] Bai Y, Tofel P, Palosaari J, Jantunen H and Juuti J 2017 *Adv. Mater.* **29** 1700767
[121] Perdew J P, Chevary J A, Vosko S H, Jackson K A, Pederson M R, Singh D J and Fiolhais C 1992 *Phys. Rev.* B **46** 6671–87
[122] Roch L M, Häse F, Kreisbeck C, Tamayo-Mendoza T, Yunker L P E, Hein J E and Aspuru-Guzik A 2018 *Sci. Robotics* **3** eaat5559
[123] Autonomous materials discovery (aimade) (http://aimade.org)